Journal of Pharmaceutical Sciences 114 (2025) 103702

Contents lists available at ScienceDirect

Journal of Pharmaceutical Sciences

journal homepage: www.jpharmsci.org

Pharmaceutics, Drug Delivery and Pharmaceutical Technology

A new model for ionizable drug dissolution in intestinal bicarbonate buffer

Jozef Al-Gousous[1,a,b,*], Adrin Jalali Sohi[1,a], Niloufar Salehi[b,c], Gordon L. Amidon[b], Peter Langguth[a]

[a] Institute of Pharmaceutical and Biomedical Sciences, Johannes Gutenberg University Mainz, Staudingerweg 5, 55128 Mainz, Germany
[b] Department of Pharmaceutical Sciences, University of Michigan, 428 Church Street, Ann Arbor, MI 48109, USA
[c] Synthetic Molecule Design & Development, Lilly Research Laboratories, Lilly Corporate Center, Eli Lilly and Company, Indianapolis, IN 46285, USA

ARTICLE INFO

Article history:
Received 10 January 2025
Revised 13 February 2025
Accepted 13 February 2025
Available online 20 February 2025

Keywords:
Dissolution
Modelling
Bicarbonate
Diffusion
Reaction

ABSTRACT

In order to achieve the desired effect *in vivo*, drugs taken orally must first be dissolved in the gastrointestinal tract. With the majority of the commercially available drugs having acidic and/or basic groups, ionization and intestinal buffering are important factors underlying adequate dissolution and, accordingly, bioavailability. The aim of this work was therefore to develop a dissolution model that properly takes these factors into account when dealing with the intestinal bicarbonate buffer. Based on the assumptions that, during dissolution, steady state is reached instantaneously, all the reactions are at equilibrium save for the interconversion between H_2CO_3 and CO_2, and diffusion of the reactants occurs over a boundary layer of a defined thickness h, a system of differential algebraic equations was developed and solved numerically using Wolfram Mathematica. The model provided very good predictions for flux values obtained from different literature sources, while involving less simplifying assumptions compared to previous models, thus enhancing its accuracy and making it a proper and promising approach for simulating dissolution in intestinal media.

Introduction

Oral dosage forms, which are usually solid, need to properly dissolve in the gastrointestinal fluids for achieving the desired bioavailability. This explains the large amount of scientific effort devoted to researching dissolution phenomena over the past decades. With the majority of drug compounds possessing acidic and/or basic groups, drug ionization is an important consideration when researching dissolution from a pharmaceutical point of view.

The recognition of the importance of ionization in drug dissolution dates back at least to 1958 when the earliest work on dissolution in reactive media was published by Higuchi et al.[1] This stagnant film model-based work opened the door to further research culminating in the seminal 1981 papers of Mooney et al.,[2,3] involving both buffered and unbuffered media. All those models assumed quasi-equilibrium throughout the boundary layer, which, given the very fast nature of proton transfer reactions, was not a bad assumption when considering a typical pharmaceutical buffer. However, when dealing with the intestinal bicarbonate-based buffer, this assumption will be problematic, for proton transfer is not the sole type of reactions occurring as shown below:

$$CO_2(aq) + H_2O(l) \rightleftharpoons H_2CO_3(aq) \rightleftharpoons H^+(aq) + HCO_3^-(aq) \quad (1)$$

The shown reactions are not limited to the very fast proton transfers. There also occurs slower interconversion of CO_2 and H_2CO_3 that must be considered. This is especially important for BCS class II acidic compounds which dissolve mainly in the small intestine. The significance of the aforementioned interconversion kinetics in dissolution was first noted by Curl in a geological context: In his 1965 paper[4], he noted that this interconversion could rate-limit the dissolution of limestone ($CaCO_3$). But this work remained unknown in the pharmaceutical field, despite the subsequent publication of some related works in the geological field.[5–7]

This issue caught more attention in the pharmaceutical field in 2014, when Krieg et al.[8] independently recognized that an equilibrium between CO_2 and H_2CO_3 in the boundary layer cannot be assumed, since the interconversion kinetics are not much faster than the diffusion kinetics under normal hydrodynamic conditions.

* Corresponding author.
E-mail address: joalgous@uni-mainz.de (J. Al-Gousous).
[1] Joint first authors

https://doi.org/10.1016/j.xphs.2025.103702

In 2019, Al-Gousous et al.[9] published the reversible non-equilibrium (RNE) model. In this model, the diffusional and reactional rates were balanced, assigning an apparent effective pK_a at which the bicarbonate system appears to buffer within the boundary layer surrounding a dissolving ionizable solute. The model was successfully validated in the rotating disk setup, applied to the particle dissolution scenario, and also used in surrogate non-bicarbonate buffer design.[10,11] When it comes to model limitations, then, in addition to those inherent to the stagnant film approach in general, this model forces the average extent of the interconversion between CO_2 and H_2CO_3 achieved in the boundary layer onto the layer's entirety. In this work, a new stagnant film-based approach (termed RNE-2), which overcomes this limitation, will be presented.

Theoretical section

Acidic drugs

For a weakly acidic monoprotic drug (HA) dissolving in bicarbonate buffer, the species of interest are HA, A^-, H^+, OH^-, H_2CO_3, CO_2 and HCO_3^-. Those species undergo the following reactions:

$$CO_2(aq) + H_2O(l) \rightleftharpoons H_2CO_3(aq) \rightleftharpoons H^+(aq) + HCO_3^-(aq) \tag{2}$$

$$K_a^{H_2CO_3} = \frac{[HCO_3^-][H^+]}{[H_2CO_3]} \tag{3}$$

$$K_{hyd} = \frac{[CO_2]}{[H_2CO_3]} = \frac{k_h}{k_d} \tag{4}$$

k_h and k_d are the first order reaction rate constants for CO_2 hydration and H_2CO_3 dehydration respectively.

$$HA(aq) + OH^-(aq) \rightleftharpoons H_2O(l) + A^-(aq) \tag{5}$$

$$HA(s) \rightleftharpoons HA(aq) \rightleftharpoons A^-(aq) + H^+(aq); \tag{6}$$

$$[HA]_0 = intrinsic\ solubility \tag{7}$$

$$K_a^{HA} = \frac{[A^-][H^+]}{[HA]} \tag{8}$$

$$H^+(aq) + OH^-(aq) \rightleftharpoons H_2O(l) \tag{9}$$

$$K_w = [OH^-][H^+] \tag{10}$$

The model assumptions are:

- Diffusion of the reactants occurring over a boundary layer of a defined thickness h (i.e. stagnant film model).
- All the reactions being at equilibrium save for the interconversion between H_2CO_3 and CO_2 which is at equilibrium only in the bulk.
- A steady state is reached instantaneously.
- The second deprotonation of carbonic acid is insignificant within the intestinal pH range

In this regard, the mass balance of the drug will be in accordance with the Mooney model[2,3]:

$$J_{HA} + J_{A^-} = p = const. \tag{11}$$

$$D_{HA}\frac{\partial[HA]}{\partial x} + D_{A^-}\frac{\partial[A^-]}{\partial x} = p = const. \tag{12}$$

with the D terms being the diffusion coefficients of the subscripted species.

Assuming D_{HA} and D_{A^-} to be equal, we get:

$$D_{HA}\left(\frac{\partial[HA]}{\partial x} + \frac{\partial[A^-]}{\partial x}\right) = p = const. \tag{13}$$

Accordingly, the concentration profile of the sum of those two species is a straight line.

$$\frac{\left([HA]_x + \frac{[HA]_x K_a^{HA}}{[H^+]_x}\right) - \left([HA]_h + [A^-]_h\right)}{(x-h)} = \frac{\left([HA]_0 + \frac{[HA]_0 K_a^{HA}}{[H^+]_0}\right) - \left([HA]_h + [A^-]_h\right)}{(0-h)} \tag{14}$$

with the unionized acidic drug species molarity at the surface ($[HA]_0$) being equal to the intrinsic solubility.

The charge balance can be written as:

$$D_{HCO_3^-}\frac{\partial[HCO_3^-]}{\partial x} + D_{OH^-}\frac{\partial[OH^-]}{\partial x} + D_{A^-}\frac{\partial[A^-]}{\partial x} = D_{H^+}\frac{\partial[H^+]}{\partial x} \tag{15}$$

Rewriting the charge balance in the algebraic form by integrating:

$$D_{HCO_3^-}[HCO_3^-]_h - D_{HCO_3^-}[HCO_3^-]_x + D_{OH^-}[OH^-]_h - D_{OH^-}[OH^-]_x + D_{A^-}[A^-]_h - D_{A^-}[A^-]_x = D_{H^+}[H^+]_h - D_{H^+}[H^+]_x \tag{16}$$

Substituting the equilibrium relationships into the previous equation (16), and assuming sink conditions for A^-, will give:

$$D_{HCO_3^-}[HCO_3^-]_h - D_{HCO_3^-}\frac{K_a^{H_2CO_3}[H_2CO_3]_x}{[H^+]_x} + D_{OH^-}\frac{K_w}{[H^+]_h} - D_{OH^-}\frac{K_w}{[H^+]_x} - D_{A^-}\frac{K_a^{HA}[HA]_x}{[H^+]_x} = D_{H^+}[H^+]_h - D_{H^+}[H^+]_x \tag{17}$$

Multiplying both sides by $[H^+]_x$ and solving the quadratic equation and taking its positive root as a solution, we get:

$$[H^+]_x = \frac{1}{2D_{H^+}[H^+]_h}\left(D_{H^+}[H^+]_h^2 - D_{HCO_3^-}[H^+]_h[HCO_3^-]_h - D_{OH^-}K_w + \left(\left(-D_{H^+}[H^+]_h^2 + D_{HCO_3^-}[H^+]_h[HCO_3^-]_h + D_{OH^-}K_w\right)^2 - 4D_{H^+}[H^+]_h\left(-D_{HCO_3^-}[H_2CO_3]_x[H^+]_h K_a^{H_2CO_3} - D_{A^-}[HA]_x[H^+]_h K_a^{HA} - D_{OH^-}[H^+]_h K_w\right)\right)^{\frac{1}{2}}\right). \tag{18}$$

The buffer mass balance can be written as:

$$D_{HCO_3^-}\frac{\partial^2[HCO_3^-]}{\partial x^2} + D_{H_2CO_3}\frac{\partial^2[H_2CO_3]}{\partial x^2} + D_{CO_2}\frac{\partial^2[CO_2]}{\partial x^2} = 0 \tag{19}$$

By integrating, and taking into account that, since there is no net source nor sink for the buffer, its total flux must be zero, we get the following expression:

$$D_{HCO_3^-}\frac{\partial[HCO_3^-]}{\partial x} + D_{H_2CO_3}\frac{\partial[H_2CO_3]}{\partial x} + D_{CO_2}\frac{\partial[CO_2]}{\partial x} = const. = 0 \tag{20}$$

After integrating, it can also be written as:

$$D_{HCO_3^-}[HCO_3^-]_x + D_{H_2CO_3}[H_2CO_3]_x + D_{CO_2}[CO_2]_x = D_{HCO_3^-}[HCO_3^-]_h + D_{H_2CO_3}[H_2CO_3]_h + D_{CO_2}[CO_2]_h \tag{21}$$

Since carbon dioxide and carbonic acid cannot be assumed to be at equilibrium, the only equilibrium relationship that can be substituted into the above equation is that relating the bicarbonate ion molarity to that of the carbonic acid resulting in the following equation:

$$D_{HCO_3^-}\frac{K_a^{H_2CO_3}[H_2CO_3]_x}{[H^+]_x} + D_{H_2CO_3}[H_2CO_3]_x + D_{CO_2}[CO_2]_x = D_{HCO_3^-}[HCO_3^-]_h + D_{H_2CO_3}[H_2CO_3]_h + D_{CO_2}[CO_2]_h \tag{22}$$

Making $[H_2CO_3]_x$ the subject of the formula for Eq. 22 and $[HA]_x$ for Eq. 14 (and assuming sink conditions there) and substituting into Eq. 18 will give us:

$$[H^+]_x = \frac{1}{2\,D_{H^+}[H^+]_h}\left(D_{H^+}[H^+]_h^{\,2} - D_{HCO_3^-}[H^+]_h[HCO_3^-]_h - D_{OH^-}K_w + \left(\left(-D_{H^+}[H^+]_h^{\,2} + D_{HCO_3^-}[H^+]_h[HCO_3^-]_h + D_{OH^-}K_w\right)^2 - 4D_{H^+}[H^+]_h\left(-D_{HCO_3^-}[H^+]_x\left(\frac{[CO_2]_hD_{CO_2} - [CO_2]_xD_{CO_2} + D_{H_2CO_3}[H_2CO_3]_h + D_{HCO_3^-}[HCO_3^-]_h}{D_{H_2CO_3}[H^+]_x + D_{HCO_3^-}K_a^{H_2CO_3}}\right)\right.\right.$$
$$\left.\left.[H^+]_hK_a^{H_2CO_3} - D_{A^-}\frac{[H^+]_x\,[HA]_0\,(h-x)\left(K_a^{HA}+[H^+]_0\right)}{h\left([H^+]_x+K_a^{HA}\right)[H^+]_0}[H^+]_hK_a^{HA} - D_{OH^-}[H^+]_hK_w\right)\right)^{\frac{1}{2}}\right) \tag{23}$$

This equation has two variables: $[CO_2]_x$ and $[H^+]_x$. Since CO_2 and H_2CO_3 are not at equilibrium in the boundary layer, the second equation will be the diffusion-reaction term for CO_2 at steady state[9]:

$$D_{CO_2}\frac{\partial^2[CO_2]}{\partial x^2} = -k_d[H_2CO_3]_x + k_h[CO_2]_x \tag{24}$$

Making $[H_2CO_3]_x$ the subject of the formula for Eq. 22 and substituting into the above expression will give:

$$D_{CO_2}\frac{\partial^2[CO_2]}{\partial x^2} = -k_d\,[H^+]_x\left(\frac{[CO_2]_hD_{CO_2} - [CO_2]_xD_{CO_2} + D_{H_2CO_3}[H_2CO_3]_h + D_{HCO_3^-}[HCO_3^-]_h}{D_{H_2CO_3}[H^+]_x + D_{HCO_3^-}K_a^{H_2CO_3}}\right) + k_h[CO_2]_x \tag{25}$$

This discretization results in a system of algebraic equations that can be solved using the FindRoot command of Wolfram Mathematica (Version 14.0, Champaign, IL, USA).

Basic drugs

For a weak base, a similar derivation can be made. It just needs to be taken into account that drug dissolution and subsequent ionization obeys the following reactions:

$$B\,(s) \rightleftharpoons B\,(aq) + H^+(aq) \rightleftharpoons BH^+(aq) \tag{30}$$

$$[B]_0 = \textit{intrinsic solubility} \tag{31}$$

$$K_a^{BH^+} = \frac{[B]\,[H^+]}{[BH^+]} \tag{32}$$

As a result, the ionized form will be entered into the charge balance as a cation and following similar steps will end up giving the following expression:

$$[H^+]_x = \frac{1}{2\left(D_{H^+}[H^+]_hK_a^{BH^+} + D_{BH^+}[H^+]_h\frac{[B]_0\left([H^+]_0+K_a^{BH^+}\right)(h-x)}{h\left([H^+]_x+K_a^{BH^+}\right)}\right)}\left(D_{H^+}[H^+]_h^{\,2}K_a^{BH^+} - D_{HCO_3^-}[H^+]_h[HCO_3^-]_hK_a^{BH^+} - D_{OH^-}K_a^{BH^+}K_w + \right.$$
$$\left(\left(D_{H^+}[H^+]_h^{\,2}K_a^{BH^+} - D_{HCO_3^-}[H^+]_h[HCO_3^-]_hK_a^{BH^+} - D_{OH^-}K_a^{BH^+}K_w\right)^2 - 4\left(-D_{H^+}[H^+]_hK_a^{BH^+} - D_{BH^+}[H^+]_h\frac{[B]_0\left([H^+]_0+K_a^{BH^+}\right)(h-x)}{h\left([H^+]_x+K_a^{BH^+}\right)}\right)\right.$$
$$\left.\left.\left(D_{OH^-}[H^+]_hK_a^{BH^+}K_w + D_{HCO_3^-}[H^+]_hK_a^{BH^+}K_a^{H_2CO_3}\,[H^+]_x\left(\frac{[CO_2]_hD_{CO_2} - [CO_2]_xD_{CO_2} + D_{H_2CO_3}[H_2CO_3]_h + D_{HCO_3^-}[HCO_3^-]_h}{D_{H_2CO_3}[H^+]_x + D_{HCO_3^-}K_a^{H_2CO_3}}\right)\right)\right)^{\frac{1}{2}}\right) \tag{33}$$

Eqs. 23 and 25 form a system of two differential algebraic equations, posing a boundary value problem. The boundary conditions are:

At $x = h$:

$$[H^+]_h = \textit{known bulk proton molarity} \tag{26}$$

$$[CO_2]_h = \textit{known bulk dissolved carbon dioxide molarity} \tag{27}$$

At $x = 0$:

$$\frac{\partial[CO_2]}{\partial x} = 0 \tag{28}$$

Since none of the reactions involving CO_2 is assumed to be at equilibrium, the no flux boundary condition at x=0 can be used.[12]

For solving this system, the second derivative term for CO_2 needs to be discretized over the boundary layer using the finite difference approximation:

$$f''(x)_i \approx \frac{f(x)_{i-1} - 2f(x)_i + f(x)_{i+1}}{\delta x^2} \tag{29}$$

With the molarity of the unionized base at the surface $[B]_0$ being equal to the intrinsic solubility.

This equation can be solved together with the CO_2 diffusion reaction Eq. (25) as described for the weak acid.

For both the weak acid and the weak base scenarios, the proton molarity at the surface is used to determine the flux as follows:

$$J = \frac{D_{A^-}}{h}[HA]_0\left(1 + \frac{K_a^{HA}}{[H^+]_0}\right) \tag{34}$$

for a weak acid, and

$$J = \frac{D_{BH^+}}{h}\,[B]_0\left(1 + \frac{[H^+]_0}{K_a^{BH^+}}\right) \tag{35}$$

for a weak base.

To simulate a rotating disk setup, the boundary "film" thickness was calculated using the Levich equation:

$$h = \frac{1.612\,\sqrt[3]{D}\,\sqrt[6]{\nu}}{\sqrt{\omega}} \tag{36}$$

Where:

D is the drug diffusivity

ν is the kinematic viscosity
ω is the angular velocity

The physico-chemical parameters used in the simulations are summarized in Table 1. Regarding the angular velocity, all simulations assumed a disk rotation speed of 100 rpm (i.e. 10.47 rad/s) unless stated otherwise.

If sink conditions are not assumed then the bulk values for HA and A^- can be defined as functions of the dissolved amount, dissolution volume and bulk pH as done with the RNE-1 model by Claussen et al[10]. Since a sparged system was used in that work, the bulk bicarbonate molarity was expressed in terms of a constant dissolved CO_2 molarity and a variable bulk H^+ molarity that changes as the dissolved drug accumulates. For more details, the reader is referred to the cited Claussen et al paper.

Results and discussion

Intrinsic dissolution

As shown by Tables 2-4, the RNE-2 model provides very good predictions for flux values obtained from different literature sources, with the prediction errors being mostly below 15%, with a maximum value of 25%. The RNE-1 model on the other hand, resulted in several instances of prediction errors exceeding 30%.[9] This indicates the superiority of the RNE-2 model as it is, in contrast to the RNE-1 model, no longer restricted by generalizing the average flux ratio of CO_2 and H_2CO_3 to the entirety of the boundary layer. This can be shown in Fig. 1. While for the RNE-1 model, the CO_2 and H_2CO_3 concentration distance profiles show similar shapes, they are clearly different for the RNE-2 model.

Furthermore, as shown by Fig. 2, the RNE-2 model is capable of accurately predicting the effect of changing rotational speed on the flux values. The flux versus the square root of the rpm profile deviates strongly from the straight line through origin associated with a diffusion rate-limited dissolution. This has been discussed before[8,9] and is related to the H_2CO_3-CO_2 interconversion kinetics not being rapid

Table 1
A summary of the physico-chemical parameters used in the simulations (at 37°C and ionic strength of 0.15 M)

Substance	Parameter	Value	Reference
Water	K_w (M^2)	4.18×10^{-14}	10
	D_{H^+} (cm^2/s)	104.9×10^{-6}	
	D_{OH^-} (cm^2/s)	63.0×10^{-6}	
	Kinematic viscosity (cm^2/s)	0.00697	
Bicarbonate buffer	$pK_a^{H_2CO_3}$	3.30	
	k_d (s^{-1})	75.5	
	k_h (s^{-1})	0.109	9
	$D_{HCO_3^-}$ (cm^2/s)	14.6×10^{-6}	
	$D_{H_2CO_3}$ (cm^2/s)	18.08×10^{-6}	
	D_{CO_2} (cm^2/s)	24.9×10^{-6}	
Ibuprofen	Intrinsic solubility (M)	2.8×10^{-4}	
	pK_a^{HA}	4.41	
	$D_{HA} = D_{A^-}$ (cm^2/s)	7.93×10^{-6}	8
	Molecular weight (g/mol)	206.28	10
Indomethacin	Intrinsic solubility (M)	5.963×10^{-6}	9
	pK_a^{HA}	4.13	16
	$D_{HA} = D_{A^-}$ (cm^2/s)	6.8×10^{-6}	
	Molecular weight (g/mol)	357.8	
Haloperidol	Intrinsic solubility (M)	3.518×10^{-6}	
	$pK_a^{BH^+}$	8.35	9
	$D_B = D_{BH^+}$ (cm^2/s)	6.6×10^{-6}	
	Molecular weight (g/mol)	375.9	

Table 2
Flux predictions of the RNE-2 model for ibuprofen in different bicarbonate buffers.

Bulk pH	$[HCO_3^-]$ (mM)	Flux ($\mu g\ cm^{-2}\ min^{-1}$)				%PE
		Theoretical	Experimental			
			Al-Gousous et al[9]	Krieg et al[8]	Average	
6.5	5	45.59	61.0	43.7	52.35	12.91
	10	58.98	70.7	62.5	66.6	11.44
	15	68.92	81.1	74.1	77.6	11.19
6.8	5	46.25	61.7	NA	61.7	25.04
	10	60.11	69.4	NA	69.4	13.39
	15	70.49	82.7	NA	82.7	14.76

Table 3
Flux predictions of the RNE-2 model for indomethacin in different bicarbonate buffers.

Bulk pH	$[HCO_3^-]$ (mM)	Flux ($\mu g\ cm^{-2}\ min^{-1}$)					%PE
		Theoretical	Experimental				
			Al-Gousous et al[9]	Krieg et al[8]	McNamara et al[13]	Average	
6.5	5	11.20	14.7	10.8	NA	12.75	12.16
	10	14.40	14.8	12.7	NA	13.75	4.73
	15	16.69	19.7	15.7	NA	17.7	5.71
6.8	5	12.00	15.4	NA	NA	15.4	22.08
	6.3	13.10	NA	NA	14.8	14.8	11.49
	10	15.71	15.7	NA	NA	15.7	0.06
	12.9	17.40	NA	NA	21.9	21.9	20.55
	15	18.50	21.9	NA	NA	21.9	15.53
	19.2	20.45	NA	NA	22.8	22.8	10.31
	25.8	23.06	NA	NA	25.8	25.8	10.62

Table 4
Flux predictions of the RNE-2 model for haloperidol in different bicarbonate buffers.

Bulk pH	$[HCO_3^-]$ (mM)	Flux ($\mu g\ cm^{-2}\ min^{-1}$)		%PE
		Theoretical	Experimental Krieg et al[8]	
6.5	5	2.91	3.58	18.72
	10	3.95	4.79	17.54
	15	4.69	5.41	13.31

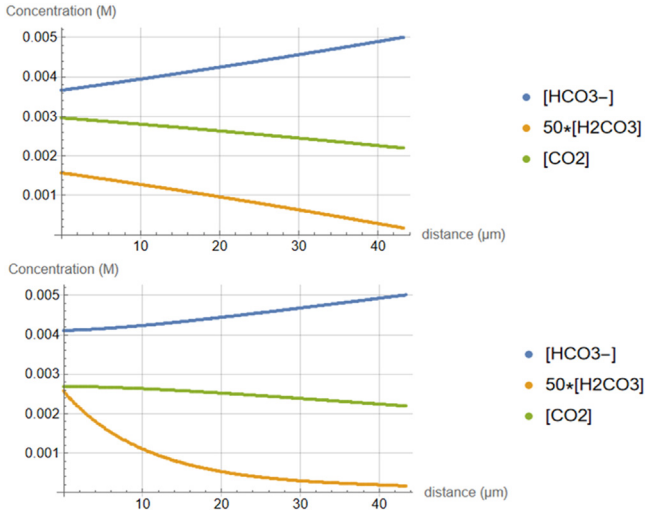

Fig. 1. Concentration profiles of the different carbon dioxide species in the boundary layer according to RNE-1 (top) and RNE-2 (bottom) models (ibuprofen in 5 mM bicarbonate pH 6.5). Number of discretization steps = 250.

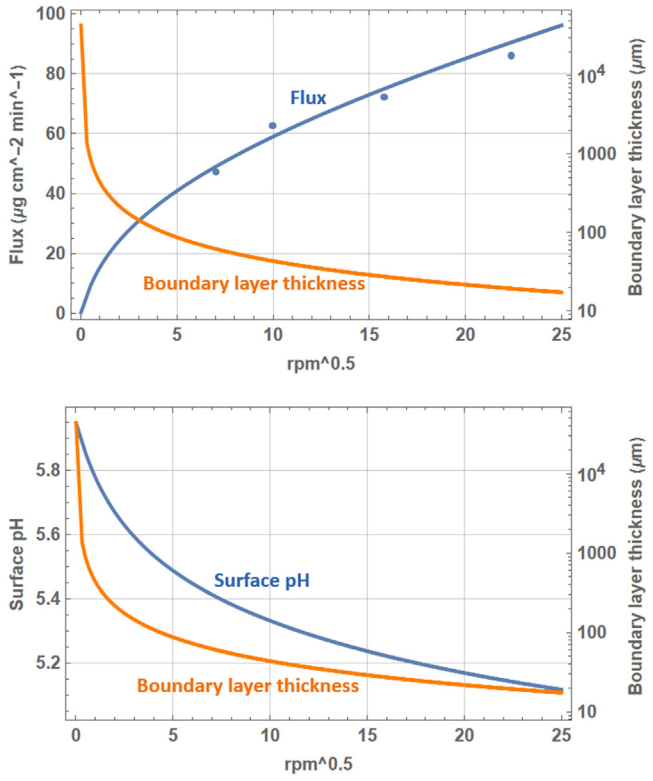

Fig. 2. Top: Predicted (curve) vs. observed[8] (dots) rpm-dependence of ibuprofen flux in 10 mM pH 6.5 bicarbonate buffer in a rotating disk setup. Bottom: Predicted surface pH values as a function of rpm. Both plots also show the effect of rpm on the boundary layer thickness. Number of discretization steps = 500.

enough to achieve equilibrium at the interface within typical diffusional times. As a result, faster rotational speeds give less time for equilibration and accordingly lead to lower surface pH-values (for weak acid dissolution) and to higher ones for a weak base. This is in line with previous research on bicarbonate.[8,9] An implication of this boundary layer thickness-dependence is a particle-size dependence of the surface pH (during suspended particle dissolution) brought about by the effect of the particle size on the boundary layer thickness as illustrated by Fig. 3.

Particle dissolution

To validate the model for the particle dissolution scenario, RNE-1 was replaced with RNE-2 in the calculations of Claussen et al[10] (which predicted the dissolution of suspended ibuprofen particles in bicarbonate buffer), and the curve shown in Fig. 4 resulted. The maximum relative prediction error decreased from 16% to 10%. Instead of this maximum prediction error appearing at the first point, it appeared at the 30-minute time point. Actually, the first three timepoints (representing the dissolution of the first 60% of the dose) were very well predicted, with the prediction error becoming higher afterwards (but still not exceeding 10%). This might be because the finer portion of the ibuprofen particles is the earlier dissolving one and with its "boundary layer thickness" being close to the particle radius, there will be less deviation from reality in terms of the assumed hydrodynamic model. As a result, the boundary layer thickness calculations for those early data points may be more robust than for the later ones. An additional potential factor here is the margin of inaccuracy present in the laser diffractometry-based particle size determination method used by Claussen et al.

The dissolution-solubility mismatch demonstrated by Claussen et al.[10] (where a large difference was found between the saturation solubility and the initial total surface concentration of the drug during dissolution in bicarbonate) is also predicted by this model. This mismatch raises a question about defining the threshold for sink conditions. Typically, sink conditions are presumed to be maintained as long as the bulk concentration does not exceed 10% of the saturation solubility. This was based on the assumption of the surface concentration being similar to the saturation solubility. However, this assumption does not hold for bicarbonate buffer. For instance, the median initial total surface drug concentration (median because different particle size fractions have different surface-pH values) of the tested ibuprofen particles is 30% of the saturation solubility in 5 mM pH 6.8 bicarbonate buffer. Accordingly, it is more accurate to take the calculated surface pH into account when estimating the sink conditions threshold during dissolution in bicarbonate buffer.

Limitations

The residual limitations of this new model are those inherent to all stagnant film models, with the assumption of all the species behaving as if they all were diffusing through a stagnant film with a well-defined thickness. As for the equilibrium assumption for the proton transfer reactions, this very commonly made assumption should have a very minor impact owing to the extremely fast nature of those reactions.

While, because of being less assumption-burdened, the RNE-2 model can provide predictions generally superior to those of RNE-1 model, it has a disadvantage of higher mathematical complexity that could potentially load to greater computational load when applied to more complicated modelling scenarios. In addition, the simplicity of

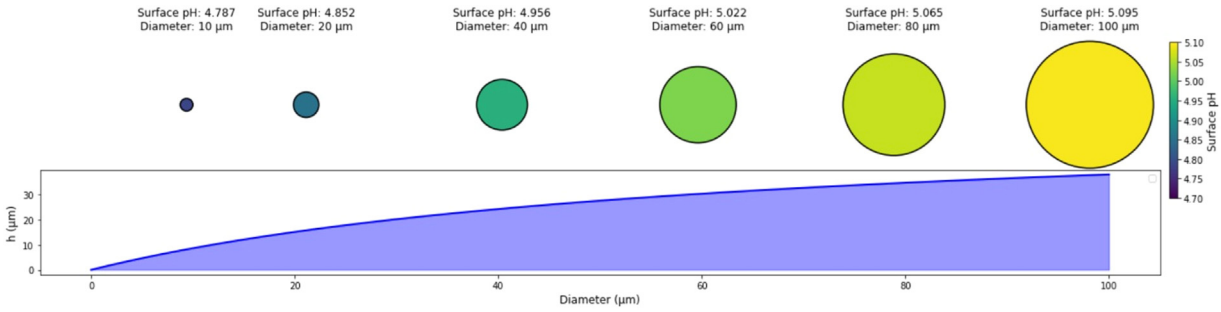

Fig. 3. Particle size-dependence of the surface pH of spherical ibuprofen particles in 5 mM pH 6.5 bicarbonate buffer (paddle apparatus at 50 rpm). For the boundary layer calculation, the adaptation of Avdeef et al.[14] of the Wang-Flannagan model[15] was used to include convection effects. Since Wang-Flannagan model essentially gives a resistance to mass transfer equivalent to the thickness of a flat boundary layer, no change of the diffusional term in Eq. 24 to the sphere version of Fick's second law is needed. Number of discretization steps = 250.

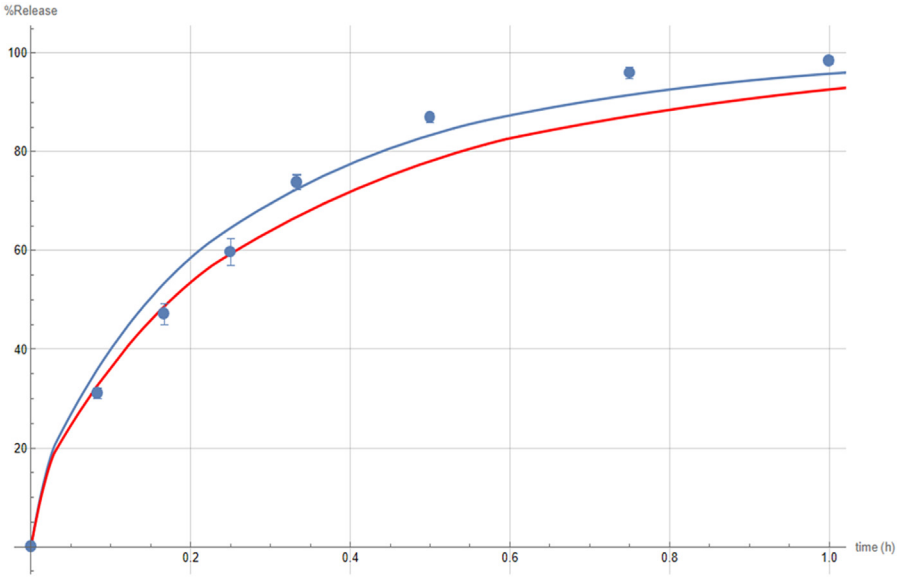

Fig. 4. Predicted (solid curves) vs. observed (dots) dissolution of suspended ibuprofen particles in 5 mM pH 6.8 bicarbonate buffer. The blue curve shows the predictions based on the RNE-1 model and the red one shows those based on the RNE-2. Number of discretization steps = 250.

RNE-1 allows the calculation of the effective pKa parameter as outlined by Al-Gousous et al.[9] which provides a very straightforward way of describing the balance between diffusional and reactional rates and the resulting distance from equilibrium when interpreting findings in bicarbonate.

When applying this model to the *in vivo* situation, it needs to be taken into account that, especially for poorly permeable compounds where sink conditions cannot be assumed in the intestine, there is an additional process of CO_2 exchange with the blood across the intestinal epithelium, which would need to be included as an additional differential equation.

Conclusion

In this work, we have succeeded in developing a new reliable model for simulating drug dissolution in intestinal bicarbonate buffer, allowing us to estimate dissolution with significantly improved accuracy. Testing the model against literature values showed lower errors for flux prediction compared to previously presented models. The remaining limitation lies in assuming a stagnant film of defined thickness, which is common to the vast majority of dissolution models, and potentially higher computational load due to increased model complexity. Nevertheless, the results provide confidence that, with this model, we have established improved foundations for an accurate simulation of drug dissolution in the intestinal tract.

Declaration of competing interest

The authors declare no conflict of interest.

Acknowledgment

We would like to thank Professor Gregory E. Amidon for the helpful discussion.

References

1. Higuchi WI, Parrott EL, Wurster DE, Higuchi T. Investigation of drug release from solids. II. Theoretical and experimental study of influences of bases and buffers on rates of dissolution of acidic solids. *J Am Pharm Assoc*. 1958;47(5):376–383.
2. Mooney KG, Mintun MA, Himmelstein KJ, Stella VJ. Dissolution kinetics of carboxylic acids I: effect of pH under unbuffered conditions. *J Pharm Sci*. 1981;70(1):13–22. https://doi.org/10.1002/jps.2600700103. PMID: 7229925.
3. Mooney KG, Mintun MA, Himmelstein KJ, Stella VJ. Dissolution kinetics of carboxylic acids II: effect of buffers. *J Pharm Sci*. 1981;70(1):22–32. https://doi.org/10.1002/jps.2600700104. PMID: 7229926.
4. Curl RL. Solution kinetics of calcite. In: *Proceedings of the 4th Int. Congress of Speleology, Postojna, Yugoslavia*. 196561–66. Sept 12-26; http://hdl.handle.net/2027.42/63010.
5. Dreybrodt W, Lauckner J, Zaihua L, Svensson U, Buhmann D. The kinetics of the reaction $CO_2 + H_2O \rightarrow H^+ + HCO_3^-$ as one of the rate limiting steps for the dissolution of calcite in the system H2O–CO2–CaCO3. *Geochim Cosmochim Acta*. 1996;60(18):3375–3381. https://doi.org/10.1016/0016-7037(96)00181-0. ISSN 0016-7037.
6. Sjöberg EL, Rickard DT. Calcite dissolution kinetics: Surface speciation and the origin of the variable pH dependence. *Chem Geol*. 1984;42(1–4):119–136. https://doi.org/10.1016/0009-2541(84)90009-3. ISSN 0009-2541.
7. Zaihua L, Dreybrod W. Dissolution kinetics of calcium carbonate minerals in H2O–CO2 solutions in turbulent flow: the role of the diffusion boundary layer and the slow reaction $H_2O + CO_2 \rightarrow H^+ + HCO_3^-$. *Geochim Cosmochim Acta*. 1997;61(14):2879–2889. https://doi.org/10.1016/S0016-7037(97)00143-9. ISSN 0016-7037.
8. Krieg BJ, Taghavi SM, Amidon GL, Amidon GE. *In Vivo* predictive dissolution: transport analysis of the CO_2, bicarbonate *In Vivo* buffer system. *J Pharm Sci*. 2014;103(11):3473–3490. https://doi.org/10.1002/jps.24108.
9. Al-Gousous J, Salehi N, Amidon GE, Ziff RM, Langguth P, Amidon GL. Mass transport analysis of bicarbonate buffer: effect of the CO_2–$H2CO_3$ hydration–dehydration kinetics in the fluid boundary layer and the apparent effective pKa controlling dissolution of acids and bases. *Mol Pharm*. 2019;16(6):2626–2635. https://doi.org/10.1021/acs.molpharmaceut.9b00187.
10. Claussen F, Al-Gousous J, Salehi N, Garcia MA, Amidon GL, Langguth P. Solubility vs dissolution in physiological bicarbonate buffer. *Pharm Res*. 2024;41(5):937–945. https://doi.org/10.1007/s11095-024-03702-5. May.
11. Hofmann M, García MA, Al-Gousous J, Ruiz-Picazo A, Thieringer F, Nguyen MA, Månsson W, Galle PR, Langguth P. In vitro prediction of in vivo absorption of ibuprofen from suspensions through rational choice of dissolution conditions. *Eur J Pharm Biopharm*. 2020;149:229–237. https://doi.org/10.1016/j.ejpb.2020.02.009.
12. Ozturk SS, Dressman JB, Palsson BO. On the use of the quasi-equilibrium assumption for drug dissolution. *Pharm Res*. 1990;7:425–429. https://doi.org/10.1023/A:1015892011092.
13. McNamara DP, Whitney KM, Goss SL. Use of a physiologic bicarbonate buffer system for dissolution characterization of ionizable drugs. *Pharm Res*. 2003;20(10):1641–1646. https://doi.org/10.1023/a:1026147620304.
14. Avdeef A, Tsinman K, Tsinman O, Sun N, Voloboy D. Miniaturization of powder dissolution measurement and estimation of particle size. *Chem Biodivers*. 2009;6:1796–1811. https://doi.org/10.1002/cbdv.200900082.
15. Wang J, Flanagan DR. General solution for diffusion-controlled dissolution of spherical particles. 1. Theory. *J Pharm Sci*. 1999;88:731–738.
16. Sun N, Avdeef A. Biorelevant pK_a (37°C) predicted from the 2D structure of the molecule and its pK_a at 25°C. *J Pharm Biomed Anal*. 2011;56:173–182.